

# Understanding Finite-State Representations of Recurrent Policy Networks

**Mohamad H. Danesh**  
Oregon State University  
daneshm@oregonstate.edu

**Anurag Koul**  
Oregon State University  
koula@oregonstate.edu

**Alan Fern**  
Oregon State University  
afern@oregonstate.edu

**Saeed Khorram**  
Oregon State University  
khorrams@oregonstate.edu

## Abstract

We introduce an approach for understanding finite-state machine (FSM) representations of recurrent policy networks. Recent work focused on minimizing FSMs to gain high-level insight, however, minimization can obscure a deeper understanding by merging states that are semantically distinct. Conversely, our approach starts with an unminimized machine and applies more-interpretable reductions that preserve the key decision points of the policy. We also contribute a saliency tool to attain a deeper understanding of the role of observations in the decisions. Our case studies on policies from 7 Atari games and 3 control benchmarks demonstrate that the approach can reveal insights that have not been noticed in prior work.

## 1 Introduction

Deep networks have been shown to be a powerful policy representation for sequential-decision making, by achieving state-of-the-art performance in both reinforcement learning [14, 8, 21, 20] and imitation learning [9]. Typically, however, there is little semantic understanding of how the learned policy networks make their decisions, which restricts their use to low-stake applications. Lack of transparency is particularly problematic for policies based on recurrent neural networks (e.g. LSTMs and GRUs [10, 5, 4]), which often yields state-of-the-art performance by conditioning decisions on hidden memory states. Since memory states are high-dimensional vectors with no preconceived semantics, it is unclear how to best interpret the memory’s role in decision making.

A recent approach for understanding recurrent policy networks is to quantize the representations of memory and observations within the RNN [12]. The quantized RNN can be viewed as an FSM, known as a Moore Machine (MM), which can be visualized and analyzed. In particular, the originally large MMs were minimized using equivalence-preserving minimization, resulting in small machines for a variety of domains, including Atari, which yielded high-level insights. For example, the minimal machine for Atari Pong showed that memory was not actually needed (i.e. a state-action mapping), while an MM extracted for Atari Bowling was an open-loop strategy that ignored the observations.

We have found that gaining more in-depth insight from minimal MMs is difficult. For example, the minimization approach allowed for determining global properties, such as whether or not the policy uses memory and/or observations in a significant way. However, gaining a more refined understanding of how observations influence the machine’s decisions is unclear based on minimal machines. As an analogy, if a human aims to write a minimal-size program for a problem, the resulting program will likely be difficult for others to understand. Instead, understandable programs will rarely be minimal, in order to explicitly expose the decision logic and structure.

Similarly, a minimal MM can hide the decision logic of the original MM. To see this, Figure 4 shows minimal MMs for Pong and Bowling and Figure 5 shows a set of frames/observations for each MM

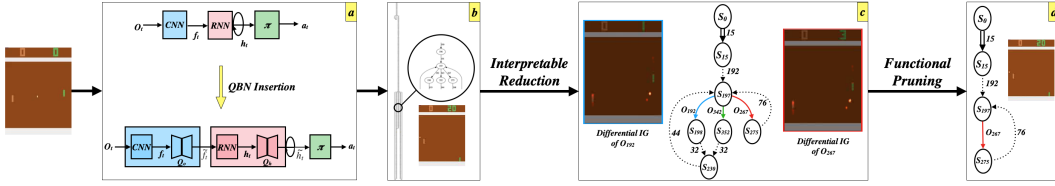


**Figure 1:** Overall approach for Pong. a) *QBN Insertion* (Section 3) discretizes observations and memory of the original RNN (top). b) Resulting *Moore Machine* with finite states and observations. c) *Interpretable reductions* (Section 4.1) are applied to the machine, yielding a single decision point  $s_{197}$  conditioning on observations. *Differential saliency* (Section 4.2) is used to understand decisions in terms of observations. d) *Functional pruning* (Section 4.3) removes unnecessary branches, which, here, leaves an open-loop policy.

that all map to a single state in the corresponding MM. For a human, the frames are semantically distinct, whereas the minimization process was able to merge them all into a single state. This is due to the minimization focusing on logical equivalence, rather than maintaining any semantic meaning of states. Thus, we have found it very difficult to understand the strategic role of different states in such MMs to gain deeper insight into their decision logic. This experience led us to the view that minimal MMs are unlikely to be a good starting point for interpreting recurrent policies.

Our main contribution is to develop a new approach to analyze MM policy representations. We demonstrate that this approach can yield significantly more insight into the decision making of recurrent policies. Rather than start with a minimal MM after quantization, we start with the unminimized MM, which is often quite large, and apply “interpretable reductions” in order to reduce the visual complexity. The reductions are straightforward in order to preserve the inherent structure, but effective, and include simple operations such as replacing a fixed series of non-branching memory states (i.e. a macro) with a single abstract transition that represents the series. The result is a simplified machine with a fixed set of “branching states” where the flow of the machine depends on observations.

In order to understand the decisions made at branching states, we further develop a new differential saliency tool, aiming to identify parts of observations that are most important for selecting one branch over another. Using the tool, we found that often, especially in Atari, the saliencies were unintuitive from a strategic point of view, which led us to question the whether observations were used for strategically important reasons, or whether they were “arbitrary” branches. This led us to consider the “functional pruning” reduction to assess that issue.

We explore this approach on 7 deterministic Atari games and 3 continuous control environments. We present both qualitative and quantitative (appendix) analyses through a number of non-trivial case studies and reveal some apriori surprising characteristics of the recurrent policies, which have been previously unnoticed. Most striking is the role that observations play in the policies learned for our Atari games. While prior work has attempted to understand the most salient pixels for policy decisions in Atari games [6, 11, 7], little insight was gained into how that information was used by the policy. Our approach reveals that, for the Atari policies, observations were not used in semantically meaningful ways and were not essential to the performance of the policy. In particular, at each branching state, it was possible to remove all branches, except for one, resulting in an open-loop policy that ignores observations, while maintaining performance. We call such policies, *pruned open-loop policies*, and observe that all of our Atari policies are of this type. Also, we show that the approach has utility for stochastic control tasks. Finally, we identify limits of the current approach as problems become larger and more stochastic, which suggests avenues of future work.

## 2 Related work

**Saliency Maps.** Saliency maps have been used as a tool to identify the most relevant parts of the input with respect to the agent’s decision [6, 11, 7, 1]. Perturbation-based saliency methods have been investigated to gain insight into learned Atari policies [6, 11, 7], but have been criticized for relying on the application of networks to potentially non-sensical perturbed states [1]. This has been partly addressed by using more advanced counterfactual state generation [16]. In general, saliency approaches produce a “local explanation” for the decisions made at specific states, which is in contrast to “global explanations” we primarily focus on in this work. Saliency methods are also limited in the type of insights they can provide. For example, while they are applied to recurrent policies, they provide no insight into how memory is used and the strategic role of salient inputs. As we will see our results suggest that a humans intuition about the role of salient inputs can be highly misleading.

**Hybrid Architectures.** There have been efforts to induce explanations components in the architecture to make RL agents implicitly explainable [24, 15]. As an example, soft attention modules have been used in a recurrent architecture to gain insight into the “attention” of an RL agent [15]. While

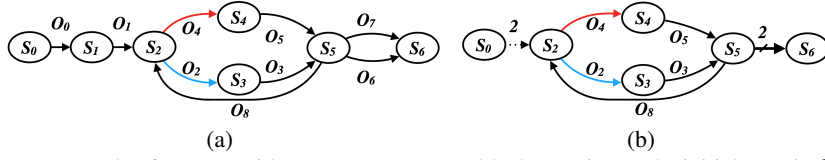


**Figure 2:** a) An example of an MM with 7 memory states and 9 observations. The initial state is  $S_0$ , and based on the input observation, it goes to the next state until it reaches to the state,  $S_5$ , then it loops back to  $S_2$ . In this example, MM has a decision point at  $S_2$ . b) Interpretable reductions applied to the MM.

attention has been used in several context for explanation, the soundness of this approach is not clear. In particular, the attention weights are computed from the raw observations and memory, which is ignored in the explanation process. Thus, it is difficult to determine whether the attention patterns carry key strategic information based on other parts of the raw observation, or whether, indeed, it is only the information highlighted by the attention that is key to decisions. Investigating ways to distinguish these two cases is interesting future work.

**Extracting Finite-State Machine.** There has been significant prior work on extracting FSMs from RNNs in the context of formal language learning of fixed finite alphabets [19, 3, 22, 23]. Only recently have there been attempts to learn FSMs for complex RL problems [12] where machine minimization was used to extract high-level insights. Our work builds on [12] and aims to significantly advance the depth of understanding that such methods can provide.

### 3 Recurrent networks to Moore Machines

In this section we review *recurrent policy networks (RPNs)* and how they can be converted to *MMs* as illustrated in Figure 1a. This work is agnostic about how a policy is learned, which, for example, could be via RL, imitation learning, or other training approaches.

**Recurrent Policy Networks (RPNs).** An RPN is an RNN policy that, at each time step, is given an observation  $o_t$  and outputs an action  $a_t$  to take in the environment. As illustrated in Figure 1a top, during execution, an RPN maintains a continuous-valued hidden memory state  $h_t$ , which is updated on each transition and influences the action choice  $a_t$ . Specifically, given current observation  $o_t$  and current state  $h_t$ , RPN outputs an action  $a_t = \pi(h_t)$  where  $\pi$  may be a feed-forward network. Then, it updates the state according to  $h_{t+1} = \delta(f_t, h_t)$ , where  $f_t$  is a set of features extracted from  $o_t$ , for example, using a CNN when observations are images.  $\delta$  is the transition function, which is often implemented via different types of gating networks such as LSTMs or GRUs.

**Moore Machines.** Understanding action choices of an RPN is complicated by the memory’s high-dimensionality and lack of predefined semantics. Recent work [12] has attempted to address this issue by transforming RPNs to *MMs*, which allows for visualization and analysis of a finite system. An MM is a finite-state machine defined by a finite set of labeled hidden states  $H$ , a distinguished initial state  $h_0 \in H$ , a finite set of observation symbols  $O$ , and a transition function  $\Delta : H \times O \rightarrow H$ , which returns the next state  $h_{t+1} = \Delta(h_t, o_t)$ , given the current state and observation symbol. The label associated with each state corresponds to an action. An MM policy initializes the state to  $h_0$  and then updates the state as observations arrive and outputs the action associated with each state.

**Quantized Bottleneck Insertion (QBN Insertion).** We now overview the approach of *Quantized Bottleneck Insertion* [12] for transforming an RPN to an MM policy, which is illustrated in Figure 1a bottom. Full details of this approach can be found in the original paper and are not critical to the contributions of this paper. The key components of the approach are *Quantized Bottleneck Networks (QBNs)*, which are simply auto-encoders, for which the encoder produces a quantized latent representation. In this work, bottleneck representation is composed of discrete units with output values in  $\{-1, 0, 1\}$ . Given a trained RPN, a representative set of RPN trajectories is produced and the resulting sets of hidden states  $\{h_t\}$  and observation features  $\{f_t\}$  are collected. Next, a hidden-state QBN  $Q_h$  and observation QBN  $Q_o$  are trained to minimize reconstruction error on the data sets. The encoders of  $Q_h$  and  $Q_o$  can be viewed as discretizing the state and observation spaces. The trained QBNs are then inserted into the RPN in place of the “wires” that propagate the continuous memory vector  $h_t$  and observation features  $f_t$  (see Figure 1a). This creates a discrete representation of the hidden states  $\hat{h}_t$  and observation features  $\hat{f}_t$  in the RPN. In practice, QBNs have reconstruction errors, which may impact the RPN performance. Supervised fine-tuning of the discretized RPN can be used to improve performance via imitation learning with respect to the original RPN.

Trajectories of the discretized RPN are then run to collect a representative transition set  $\{(\hat{h}_t, a_t, \hat{f}_t, \hat{h}_{t+1})\}$ , indicating that action  $a_t$  was taken in discrete state  $\hat{h}_t$  and that a transition to  $\hat{h}_{t+1}$  was observed when the discrete observation was  $\hat{f}_t$ . The MM is constructed by creating a

transition graph edge for each data tuple. The key parameters relevant to this paper are the sizes of the bottlenecks of  $Q_h$  and  $Q_o$ , denoted  $N_h$  and  $N_o$  respectively. Larger values give more potential to produce finer grained quantization and in turn more states.

## 4 Analyzing non-minimal Moore Machines

RPNs learned for complex problems can result in MMs with large numbers of discrete states and observations. In order to aid understanding, previous work [12] used a standard minimization algorithm [17] to produce equivalent minimal state MMs. As described in Section 1, the minimal machines allowed for interesting global insights into the general use of states and observations. However, as also described in Section 1, we have found that minimal MMs obscure the decision making behavior, since they compress the original MM structure with no regard for interpretability. For example, the observations mapped to single states often appear to be semantically very different (Figure 5), making it difficult to understanding the role of states and how observations influence their choices. Thus, in this paper, we start with the unminimized MMs with the aim to gain a more detailed understanding. Below, we describe the steps of our analysis approach.

### 4.1 Interpretable Reductions

Figure 2a shows an example MM, which illustrates the main structures we observed in the learned MMs we analyzed. These structures provide several opportunities for simple *interpretable reductions*, which simplify the visualization of an MM without obscuring decision structure. The reductions are very simple one of our contributions is to notice that this simple set can be effective for interpreting very large MMs. The first stage of our approach applies the following interpretable reductions.

**Sequence Reduction.** It is common to see long sequences of states with a single observation between consecutive states (e.g.  $S_0$  to  $S_2$  in Figure 2a). These sequences are open open-loop macros that simply execute a fixed sequence of actions whenever encountered. Examples are  $S_0$  and  $S_1$  in the sequence of state-transitions from state  $S_0$  to  $S_2$  that have no branching states. We reduce these sequences to a single “macro arc” represented as a dotted line with a number indicating its length.

**Loop Unrolling Reduction.** There are many loops attached to sequences that are only traversed once when the sequence is visited. These loops increase the visual complexity of the MMs, so we we unroll such loops before applying sequence reduction.

**Parallel Reduction.** There are often multiple transition arcs between two states with different observation labels (e.g. between  $S_5$  and  $S_6$  in Figure 2a). This can also occur for self-transitions. We merge these arcs into an abstract arc labeled by the number of number of observations.

**Startup and Termination Reduction.** In some MMs, there is a period of state transitions that corresponds to a warm-up/termination period in the environment where actions have no impact. If desired, these parts of an MM can be replaced with a macro arc represented by two parallel lines with the number of transitions in that period. This reduction requires minimal human annotation of the steps where episodes “meaningfully” begin and end, which is usually straightforward.

The result of these reductions is shown in Figure 2b and often result in orders of magnitude smaller visualizations, e.g., going from Figure 1b to Figure 1c). Note that interpretable reductions do not change the behavior of the agent, nor the control flow, but are only for improved visualization. The states remaining in the reduced diagram are *decision points* (e.g. state  $S_2$  is the single decision point in Figure 2b), where the next state, and hence future behavior, depends on the observation. The decision points are the key states in the machine that dictate how its behavior is influenced by observations. It is these points where we can gain the most insight about an MM.

### 4.2 Differential Saliency for Decision Points

Given an MM decision point, we are interested in understanding how the raw observations (e.g. image pixels) influence its decisions. In particular, for a pair of outgoing branches labeled by discrete observation  $\hat{o}_1$  and  $\hat{o}_2$ , we would like to answer the question: “*What features of the raw observations are most influential to selecting the  $\hat{o}_1$  branch versus  $\hat{o}_2$ ?*”. To help answer this, we consider pairs of raw observations  $o_1$  and  $o_2$  that occur at the decision point during MM execution (e.g.  $o_{342}$  and  $o_{267}$  in Figure 1c), such that  $\hat{o}_i = E_o(o_i)$ . That is,  $o_1$  and  $o_2$  are example observations that cause the machine to differentiate between the branches. We then produce a *differential saliency map*  $S(o_1, o_2)$  that highlights the parts of  $o_1$  and  $o_2$  that are most responsible for preferring branch  $\hat{o}_1$  over  $\hat{o}_2$ . To compute  $S(o_1, o_2)$ , we focus on the set  $F(o_1, o_2)$  of discrete features produced by  $E_o$

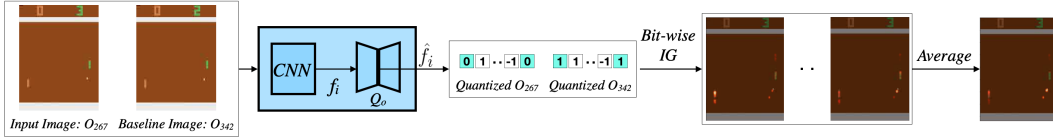


**Figure 3:** Differential Saliency Pipeline. The pair of images under comparison result in discrete representations that differ on the highlighted features. We produce a saliency map for each of those features using the Integrated Gradient (IG) approach and average the magnitude of the maps for an overall differential saliency map.

that differ between  $o_1$  and  $o_2$ . For each  $f \in F(o_1, o_2)$  we first produce a saliency map  $S[f](o_1, o_2)$  that highlights the parts of  $o_1$  and  $o_2$  that “explain” the difference in value of  $f$ .  $S(o_1, o_2)$  is then just the average of the individual maps. Source code is provided in the appendix.

We compute each  $S[f](o_1, o_2)$  via a straightforward, but novel, adaptation of the *Integrated Gradient* (IG) saliency approach [18]. Originally, IG was used to compute saliency maps that explain the decision of a classifier on a single image/observation  $o$ . Fundamental to the approach is the notion of a *baseline* image  $o_b$ , which is used as a reference that is assumed to not excite the classifier. In an image domain, the baseline is often a constant or noise image. Let  $f(o)$  be the classifier response for observation  $o$  (usually the largest class-specific input to the softmax layer), noting that  $f(o_b)$  will be small, and let  $IG_i[f](o, o_b)$  be the corresponding saliency value produced by IG for feature/pixel  $i$ . The key property of IG, which makes it a meaningful notion of saliency, is the relation  $\sum_i IG_i[f](o, o_b) = f(o) - f(o_b)$ . Thus, the saliency value of pixel  $i$  can be viewed as its additive contribution to the difference in classification responses for  $O$  over  $O_b$ . For space reasons we refer the reader to the original paper [18] for the details of the IG computation.

As illustrated in Figure 3, we adapt IG to compute our differential saliency maps  $S[f](o_1, o_2)$  by treating  $o_2$  as the baseline and letting the response functions  $f \in F(o_1, o_2)$  be the continuous features computed by the encoder just before the discretization step. That is, differential saliency is given by  $S[f](o_1, o_2) = IG[f](o_1, o_2)$ . This means that differential saliency satisfies  $\sum_i S_i[f](o_1, o_2) = f(o_1) - f(o_2)$ , which has the clear interpretation that each saliency value  $S_j[f]$  can be viewed as an additive contribution to the difference in response for  $o_1$  and  $o_2$ , as desired.

### 4.3 Functional Pruning

After exploring the reduced MM graphs and saliency in Atari we made two high-level observations. First, as shown in our experiments the differential saliency results often indicated that observations were not being used in a strategically meaningful way, e.g., branching on observations that were extremely similar. Second, the graphs beyond different branches at a decision point were often very similar and appeared to address similar situations. We hypothesized that many decisions points may not be strategically meaningful, but rather just an artifact of learning. That is, even if a branching decision is not required at a certain point in a game, the inclusion of a decision-point that conditions on an arbitrary part of the observation will not hurt performance as long as good behavior is learned for each of the resulting branches. In such situations, the choice of which branch to traverse may be arbitrary and any one of them may work. Note that the usual saliency-based tools [6, 11, 7] will simply indicate the agent’s attention and can lead a human to incorrectly infer strategic relevance.

Detecting unnecessary decision points cannot be done by just graph analysis—rather, empirical analysis is required. To do this we conduct a simple form of *functional pruning* (details and pseudo-code in appendix), to identify and prune unnecessary branches at decision points. Our approach considers each MM decision point, prunes each of the branches one at a time, in order of the least to most frequently visited based on multiple MM runs. When a branch is pruned, we empirically estimate the performance of the resulting MM, noting that when the machine would have previously taken the pruned branch, we force it to take the most frequent branch. If the empirical performance does not degrade beyond a threshold, we permanently remove the branch and move on to the next pruning step. *The intent of function pruning is not to preserve logical equivalence*. Rather, the intent is to test whether observations were strategically important or just an artifact of learning. After gaining the insights one could decide to use the original machine or attempt to improve it.

While more sophisticated search methods over pruning combinations could be developed, we found greedy pruning to be effective for the MMs considered in this paper. For example, in Figure 1 we see that functional pruning resulted in pruning all but one branch from the single decision point in the MM, leaving an open-loop policy. In such cases, when an MM can be functionally pruned to the point of removing all decision points and leaving an open loop policy, we say that the MM is a *pruned open-loop policy*, which generalizes the notion of open-loop policy to include machines that condition on observations, but in a way that is not strategically necessary.

**Table 1:** MM statistics before and after functional pruning for control tasks and Atari environments.

Game	QBN Sizes		Before Pruning				After Pruning			
	$N_h$	$N_o$	Decis. Points	States	Obs.	Perf.	Decis. Points	States	Obs.	Perf.
Acrobot	4	4	9	12	38	-77.1	2	4	3	-80.7
CartPole	4	4	6	7	18	500	2	4	5	<b>500</b>
LunarLander	32	32	195	1426	1150	180.48	184	1387	980	172.2
Bowling	64	100	5	630	552	60	<b>0</b>	546	488	<b>60</b>
Boxing	64	100	<b>0</b>	1097	1095	100	<b>0</b>	1097	1095	<b>100</b>
Breakout	64	100	5	1659	1608	404	<b>0</b>	1598	1540	<b>404</b>
MsPacman	64	100	34	895	876	3060	<b>0</b>	776	758	<b>3080</b>
Pong	64	100	2	384	369	21	<b>0</b>	271	268	<b>21</b>
SeaQuest	64	100	18	2244	2261	2580	<b>0</b>	1834	1883	<b>2580</b>
SpaceInvaders	64	100	35	1914	1852	1820	<b>0</b>	1832	1802	<b>1820</b>

## 5 Experiments

The only prior approach to compare against is the recent MM minimization approach for analysis of MMs [12]. As described earlier, we have found it very difficult to gain insights from minimized MMs. However, to further illustrate this point, in the appendix we provide a quantitative and qualitative comparison of the MM approach to our approach in Atari games. Overall, the minimization approach is not able to reveal the interesting insights of our new approach.

We consider 7 deterministic Atari environments: Bowling, Boxing, Breakout, MsPacman, Pong, SeaQuest and SpaceInvaders, and 3 stochastic discrete-action classic control tasks: Acrobot, CartPole, and LunarLander. For each experiment, we follow the choices of prior discretization work [12] for pre-processing, RPN architecture, QBN architectures, and training via A3C reinforcement learning. Detailed information on these choices along with hyperparameter choices are in the appendix. We considered two sets of QBN sizes for each environment, but for space reasons show only one pair here in Table 1 (other results are in Appendix). From the table we see that the agent performance remains the same after reductions for all domains, except for Acrobot and LunarLander, where functional pruning reduced performance within the specified tolerance. The table also gives the number of states and observations,  $N_h$  and  $N_o$ , after the reductions. Interestingly, in Atari games, no decision points are left after functional pruning, i.e. all of the policies were “pruned open-loop” policies. The following case studies illustrate how our approach is useful for gaining insights and revealing unexpected properties of the decision logic. Additional examples are in the Appendix.

### 5.1 Atari: Case Studies

**Example Insights: Pong and Bowling.** The RPN for Pong achieved a maximum score of 21. The policy displays repetitive behavior by performing a “kill shot” against the opponent to win each point, though the behavior is not exactly the same across all shots. Figure 1b shows a view of the original large MM. Figure 1c shows the graph after the interpretable reductions, which is quite small with only one decision point at state  $S_{197}$ . This key decision point is the starting point of 3 possible loops, depending on the branch taken, and is entered once per round (each round is one point). This raised the questions of “*What basis is the machine using to decide which loop to enter?*” and “*Is there a strategic reason for the branching decision?*”.

To investigate, we computed the differential saliency for the decision of choosing  $S_{275}$  over  $S_{352}$ , as shown in Figure 3. It is striking that the sample observations associated with the branches are almost identical. The differential saliency indicates that the ball region and tips of the paddles are the most critical factors in deciding between the branches. Close inspection reveals that the appearance and location of the ball in the two observations are subtly different. To understand this we observed that these differences are due to the fact that at the beginning of each round the starting position of the ball is minutely different for even versus odd points, which translated to the small difference observed at the decision point. Intuitively this difference did not appear to have strategic value. Indeed, after functional pruning (Figure 1d) we see that all branches were removed except for the one through  $S_{275}$ , leaving an open-loop strategy with no loss in performance. The even versus odd branching, was an unnecessary artifact of the RNN learning process.

For Bowling the original large MM had 630 discrete states and 552 discrete observations. Our interpretable reductions revealed only 5 of those states corresponded to true decision points. Further, Figure 4c shows the result of functional pruning to get an MM with no loss in performance. Similar



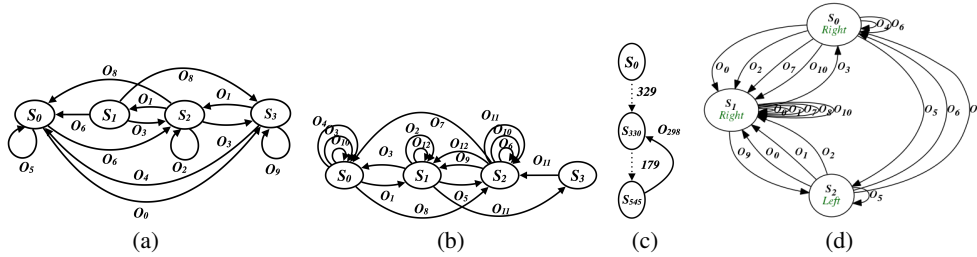


**Figure 4:** a) Pong minimal MM, b) Bowling minimal MM, c) Bowling pruned MM, d) Acrobot minimal MM.

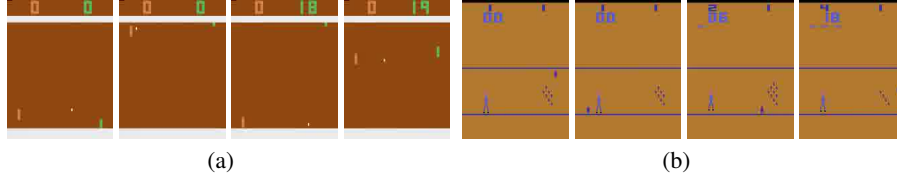


**Figure 5:** A set of four observations that enter a state in the corresponding minimal MM. a) Frames of Pong for in-going observations to  $S_2$ , b) Frames of Bowling for in-going observations to  $S_0$ .

to Pong we end up with a pruned open-loop policy. Again the observation use at decision points was not strategically relevant and rather an artifact of learning.

**Comparison to Prior Work.** We now compare our approach to the minimization approach of prior work [12]. For Pong, our approach was able to isolate a single decision point Figure 1d where behavior depended on observations in an understandable way, which was ultimately determined to be non-strategic. Rather, Figure 4a shows the minimal MM produced by prior work for the same initial MM. This minimal MM merges the key decision point with semantically unrelated states (e.g. from multiple macros), obscures insights, and gives no understanding of how memory and observations are used. To highlight this deficiency, Figure 5a demonstrates four frames of Pong which enter  $S_2$  in the corresponding minimal MM. This is an evidence of minimal MMs merging states that are semantically distinct. Further, it is unclear how the equivalent of functional pruning could be done using the minimal MM, due to the merging of decision points. It is unclear how to uncover the key insight identified by our approach by starting with the minimal MM.

A similar comparison holds for Bowling where our approach resulted in the open-loop policy in Figure **Bowling**. Rather, the minimal MM of the same initial policy is shown in Figure 4b, which resembles the tightly coupled minimal MM of Pong. Figure 5b shows frames that lead to decision point  $S_0$ , which appear to be semantically very different from a human perspective. This is also the case for other states, which makes it very difficult to extract meaningful insights from the minimal MM. Again, it is completely unclear how we could start with the minimal machine and gain the realization that the observations play no significant strategic role, which our approach revealed.

**Overall Results.** Due to page limit, qualitative comparisons of other Atari games are provided in the appendix. Nevertheless, they provide similar distinctions which show our approach’s advantage over [12]’s. Table 1, gives information about the MMs before and after functional pruning for each game. Note that 0 decision points indicates an open-loop policy. We see that before functional pruning there is only one case of open-loop policies: Boxing. All other MMs have at least one decision point. This initially makes one to believe that observations are a key part of the overall MM strategy. However, in each such case, we found that it was rare to find a decision point where observations provide strategic values at a decision point. This was confirmed by our most striking finding. After functional pruning, each of the games resulted in open-loop MMs (i.e. zero decision points). Thus, in all cases, Atari RPNs produced MM representations that were pruned open-loop policies.

## 5.2 Stochastic Classic Control Tasks

**Acrobot.** This control task includes two joints and two links, where the joint between the two links is actuated. Initially, the links are hanging downwards, and the goal is to swing the end of the lower link up to a given height. The state vector gives the sin and cos of the two rotational joint angles and the joint angular velocities. The actions involved are -1, 0 or +1 torque. We share pruned state machine for QBN sizes (4, 4) in Figure 6b. We applied our differential saliency approach to decision point  $S_2$  and found that the most important observation features were ‘sin of joint angle 1’ and ‘joint 2 velocity’. The Figure shows the scatter plot of the decisions at  $S_2$  versus these features. The plot reveals that for positive sin values, a torque of -1 is applied by stating in  $S_2$  forcing link 1 and link 2 to rise against gravity. This torque is applied until it transitions to  $S_3$  via  $O_1$  which corresponds to a positive velocity for joint 2 as shown in the scatter plot. This happens when link 2 cannot go further

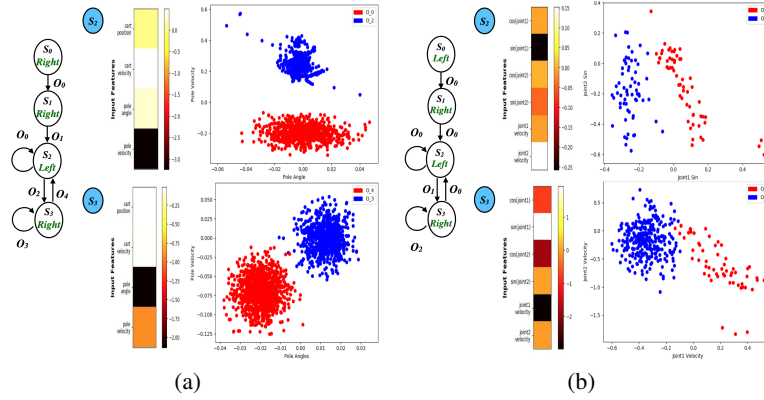


**Figure 6:** Pruned MMs for control tasks. a) CartPole, and b) Acrobot. In each case, we show saliency of features for decision points. Also, we show scatter plots of continuous observations during an episode at each decision point for the two most salient features, where color indicates the corresponding discrete machine observation.

up against gravity under the current momentum. In this state, it applies +1 torque to supplement the momentum provided by the pull of gravity. It transitions back to  $S_2$  via  $O_0$  only when the joint velocity of link 1 is positive, indicating that it cannot go further up. This loop between state  $S_2$  and  $S_3$  generates enough momentum to eventually reach the goal.

In contrast, we compare against the minimal MM (Figure 4) extracted via prior work [12]. This MM, is fully connected and merges many different types of observations. Through various previous attempts, we were unable to elicit a clear description of the machines operation. Rather, our reduction approach was able to lead to the above relatively clear understanding of the machine.

**CartPole.** We use the standard OpenAI CartPole environment with randomized initial states. Table 1 shows that the number of decision points is 6 before functional pruning and reduces to 2 after. The pruned MM is shown in Figure 6a, which has the same simple structure as for Acrobot. The machine primarily transitions between  $S_2$  (left movement) and  $S_3$  (right movement) with self-loops at those states between transitions. The figure shows the differential saliency computed over the features at  $S_2$  and  $S_3$  with the key features being “pole-velocity” followed by “pole-angle”. The scatter plots for the decisions against these features show that at  $S_2$  there is a clear threshold of positive pole-velocity that transitions to  $S_3$  to take the “right” action, and otherwise continues with “left”. This is an intuitive strategy for reducing the velocity. Similar insights are gained via the scatter plot at  $S_3$ , but here both pole-velocity and pole-angle play a role in the decision. Again, our approach was able to produce an MM that has a very clear and meaningful interpretation.

## 6 Discussion and current challenges

Our analysis is the first to provide such detailed insights into the decision making of recurrent policies trained for deterministic Atari games. Indeed, the observation that all of the considered policies resulted in pruned open-loop controllers was something that was unexpected apriori and not apparent from prior work on explaining Atari policies. For example, prior work on saliency analysis of Atari policies, even for the deterministic setting, leaves one to believe that observations play a key role in the decision making. It is tempting to discount the above insights, due to the deterministic setting, since 1) it is clear that there exist open-loop controllers for any deterministic domains, and 2) prior work has shown that search is able to find effective straight-line open-loop plans for some Atari games [2, 13]. However, these points do not imply that an RPN would necessarily learn an open-loop controller and indeed we observed that they do not. It is reasonable to expect RPNs would leverage observations in a meaningful way to get a more compact and general policy, but we instead saw the role for observations was very different and not meaningful. This demonstrates the importance of approaches that are able to concretely identify the nature of the decision making and in particular, concretely determine the role of observations to choices.

As we moved to more complex and stochastic environments, we observed that our current approach does not reveal easily analyzable machines. This was apparent in preliminary experiments with stochastic Atari. In particular, we have observed that the discrete sequences produced across different episodes have some overlap, but also are dominated by large numbers of disjoint states. Some potential explanations for this are: 1) An inadequacy of our approach—e.g., the quantization process and/or reduction steps/analysis may need to be improved; 2) Our approach may be identifying the fundamental nature of the learned RNN policies. That is, the policies may effectively use large numbers of training trajectories to encode large numbers of effectively (pruned) open-loop patterns.



As new observations are encountered the machines then map to the closest encoded patterns in a nearest neighbor style. This second possibility would suggest the need for improved RPN training approaches to support data efficiency and interpretability.

## 7 Broader impact

With the emergence of deep learning, there have always been concerns about its interpretability. Due to its black-box nature, deep learning has been limited to low-stake applications. For example, it is unknown how a model performs given previously unseen data, or the reason behind taking an action by an RL agent. Especially, in highly uncertain environments, understanding the decision-making mechanisms becomes more critical. Once we are aware of the mechanisms of these machines, we can either be more confident in deploying them or work on targeted improvements.

Our work focuses on deep RL and measures how agents utilize observations and memory. Being able to explain the behavior of agents helps deep RL to become more applicable to real world problems. Note that our paper has shown that previous approaches based on saliency techniques alone can lead to misleading understanding of the policies. For example, in Pong if the ball is highlighted by a saliency technique, a human may be satisfied that the agent is paying attention to the right thing. However, our analysis showed, that while the network was conditioning on the observation, it was doing so for meaningless reasons and might as well have been ignoring the screen. Thus, our work has helped develop a methodology for uncovering a new level of insight into recurrent policies.

## References

- [1] A. Atrey, K. Clary, and D. Jensen. Exploratory not explanatory: Counterfactual analysis of saliency maps for deep {rl}. In *International Conference on Learning Representations*, 2020.
- [2] M. G. Bellemare, Y. Naddaf, J. Veness, and M. Bowling. The arcade learning environment: An evaluation platform for general agents. *Journal of Artificial Intelligence Research*, 47:253–279, 2013.
- [3] A. L. Cechin, D. Regina, P. Simon, and K. Stertz. State automata extraction from recurrent neural nets using k-means and fuzzy clustering. In *23rd International Conference of the Chilean Computer Science Society, 2003. SCCC 2003. Proceedings.*, pages 73–78, Nov 2003.
- [4] K. Cho, B. van Merriënboer, C. Gulcehre, D. Bahdanau, F. Bougares, H. Schwenk, and Y. Bengio. Learning phrase representations using rnn encoder-decoder for statistical machine translation, 2014.
- [5] J. Chung, C. Gulcehre, K. Cho, and Y. Bengio. Empirical evaluation of gated recurrent neural networks on sequence modeling, 2014.
- [6] S. Greydanus, A. Koul, J. Dodge, and A. Fern. Visualizing and understanding Atari agents. In J. Dy and A. Krause, editors, *Proceedings of the 35th International Conference on Machine Learning*, volume 80 of *Proceedings of Machine Learning Research*, pages 1792–1801, Stockholmsmässan, Stockholm Sweden, 10–15 Jul 2018. PMLR.
- [7] P. Gupta, N. Puri, S. Verma, D. Kayastha, S. Deshmukh, B. Krishnamurthy, and S. Singh. Explain your move: Understanding agent actions using focused feature saliency. In *International Conference on Learning Representations*, 2020.
- [8] M. Hausknecht and P. Stone. Deep recurrent q-learning for partially observable mdps. In *2015 AAAI Fall Symposium Series*, 2015.
- [9] J. Ho and S. Ermon. Generative adversarial imitation learning, 2016.
- [10] S. Hochreiter and J. Schmidhuber. Long short-term memory. *Neural computation*, 9(8):1735–1780, 1997.
- [11] R. Iyer, Y. Li, H. Li, M. Lewis, R. Sundar, and K. P. Sycara. Transparency and explanation in deep reinforcement learning neural networks. *CoRR*, abs/1809.06061, 2018.
- [12] A. Koul, A. Fern, and S. Greydanus. Learning finite state representations of recurrent policy networks. In *International Conference on Learning Representations*, 2019.

- [13] M. C. Machado, M. G. Bellemare, E. Talvitie, J. Veness, M. Hausknecht, and M. Bowling. Revisiting the arcade learning environment: Evaluation protocols and open problems for general agents. *Journal of Artificial Intelligence Research*, 61:523–562, 2018.
- [14] V. Mnih, K. Kavukcuoglu, D. Silver, A. Graves, I. Antonoglou, D. Wierstra, and M. Riedmiller. Playing atari with deep reinforcement learning. *arXiv preprint arXiv:1312.5602*, 2013.
- [15] A. Mott, D. Zoran, M. Chrzanowski, D. Wierstra, and D. J. Rezende. Towards interpretable reinforcement learning using attention augmented agents. *CoRR*, abs/1906.02500, 2019.
- [16] M. L. Olson, L. Neal, F. Li, and W.-K. Wong. Counterfactual states for atari agents via generative deep learning. *arXiv preprint arXiv:1909.12969*, 2019.
- [17] M. C. Paull and S. H. Unger. Minimizing the number of states in incompletely specified sequential switching functions. *IRE Transactions on Electronic Computers*, pages 356–367, 1959.
- [18] M. Sundararajan, A. Taly, and Q. Yan. Axiomatic attribution for deep networks. In *Proceedings of the 34th International Conference on Machine Learning-Volume 70*, pages 3319–3328. JMLR. org, 2017.
- [19] P. Tiño, B. G. Horne, C. L. Giles, and P. C. Collingwood. Finite state machines and recurrent neural networks—automata and dynamical systems approaches. In *Neural networks and pattern recognition*, pages 171–219. Elsevier, 1998.
- [20] H. Van Hasselt, A. Guez, and D. Silver. Deep reinforcement learning with double q-learning. In *Thirtieth AAAI conference on artificial intelligence*, 2016.
- [21] Z. Wang, T. Schaul, M. Hessel, H. Van Hasselt, M. Lanctot, and N. De Freitas. Dueling network architectures for deep reinforcement learning. *arXiv preprint arXiv:1511.06581*, 2015.
- [22] G. Weiss, Y. Goldberg, and E. Yahav. Extracting automata from recurrent neural networks using queries and counterexamples, 2017.
- [23] G. Weiss, Y. Goldberg, and E. Yahav. Learning deterministic weighted automata with queries and counterexamples, 2019.
- [24] Z. Yang, S. Bai, L. Zhang, and P. H. S. Torr. Learn to interpret atari agents. *CoRR*, abs/1812.11276, 2018.

## 1 Functional Pruning

In this method, we perform forward parsing of the MM from the start-state to the final state. During parsing, we only consider outgoing transactions from a decision point for the purpose of pruning. Over here, each transition is weighted as per its visitation frequency which is empirically estimated by multiple runs of the MM. At each decision point, we consider each transition for pruning in the least to most frequency order. Once a transition is pruned, the overall MM is evaluated for decay in performance. During evaluation, if we encounter the pruned observation transaction, we transact through the most frequent branch of the decision point. If there is a decay in performance, the transition is restored and other candidates are considered. This simple and greedy functional pruning method is able to keep the performance, while removing unnecessary branches from the MM. Since sequence of actions at two branch may be identical, or different than one another, this type of MM minimization may change the behavior of the agent, after functional pruning. Algorithm 1 shows the pseudo-code of functional pruning.

---

### Algorithm 1: Functional Pruning

---

**Result:** Pruned MM

```

1 DecisionPoints = [];
2 PrunedBranches = [];
3 for node in (Nodes in MM) do
4   if node is decision point then
5     | DecisionPoints.append(node and frequency);
6   end
7 end
8 for DP in DecisionPoints do
9   leastFreqBranch = the least frequent branch;
10  mostFreqBranch = the most frequent branch;
11  new MM = prune leastFreqDP from MM;
12  for node in new MM do
13    if node is in leastFreqBranch then
14      | node = mostFreqBranch;
15    end
16  end
17  performance = record the performance of new MM;
18  if performance unchanged then
19    | PrunedBranches.append(leastFreqBranch);
20  end
21 end
22 for PB in PrunedBranches do
23   | remove PB from MM;
24 end
25 Return MM

```

---

## 2 Differential IG

Source code is publicly available over here: <https://tinyurl.com/rofwbbm>. It is uploaded to Google drive as a .tar.gz file for the sake of anonymity. Once decisions are out, we will put it on GitHub.

## 3 Pre-processing

In Atari games, input images are pre-processed. This has been done by applying a wrapper over OpenAI gym environments which gray-scales and resizes input images from  $210 \times 160$  to  $80 \times 80$  shape. Also, We use deterministic Atari environments with *frameskip* = 4. For Pong and SpaceInvaders, we changed the action space to [Noop, RightFire, LeftFire] and [Noop, Fire, Right, Left], respectively. These pre-processing steps are done in order to ease policy training and interpretation.

In classic control tasks, we do not exert any pre-processing on input features and action spaces.

## 25 4 Training Details

26 We used A3C with Adam optimizer ( $lr = 1e - 4$ ) to train our Recurrent Policy Network(RPN).  
27 Also, we used discount= 0.99 and calculated policy loss using Generalized Advantage Estimation  
28 (GAE)( $\lambda = 1.0$ ).

29 **Atari.** In this case, RPN comprises of 4 convolutional layers (kernel size 3, strides 2, padding 1, and  
30 32, 32, 16, 8 filters respectively) with intermediate ReLU activations. The last convolutional layer  
31 has ReLU6. This is followed by a GRU Cell having 32 hidden units. The output of GRU is consumed  
32 by a "policy" and "value" linear network having 'action-space' and '1' unit, respectively.

33 **Continuous Control Tasks.** RPN is composed of 2 linear layers having 16 and 8 units, respectively.  
34 First layer's activation function is ELU and second layer's is ReLU6. Rest of the architecture is same  
35 as for Atari.

36 **QBNs.** Each QBN comprises of 'n' layer encoder and 'n' layer decoder. At the bottleneck, we used  
37 the same *TernaryTanh* operator to quantize the encoded representation as done in prior work. This  
38 quantized representation is fed to the decoder. Also, We used Tanh as intermediate activation's for  
39 encoder and decoder. We used  $n = 2$  and  $n = 3$  and apply ReLU6, Tanh activation to last layers of  
40  $Q_o$  and  $Q_h$ , respectively. In each QBN's encoder, for the first layer there are  $8 \times QBN\ SIZE$  neurons,  
41 and for the second layer there are  $4 \times QBN\ SIZE$  neurons. In the final layer there are  $QBN\ SIZE$   
42 neurons. For QBN's decoder, the order is reversed. We use Adam optimizer ( $lr = 1e - 4$ ) and max  
43 norm of the gradients was set to 5.

## 44 5 Quantitative analyses

45 Table 1 provides the results of original MM, minimal MM, and our approach, for two QBN pairs.  
46 For either pair, our results are consistent, and agent with the pruned MM performs the same as the  
47 original agent, except for Acrobot and LunarLander. In those two environments, we have a small  
48 drop in performance, but agent is still able to solve the problem. We have not included the detailed  
49 information about each interpretable reduction step, Section 4.1, since their purpose is to make  
50 visualization simpler. The underlying MM would not change by applying interpretable reductions,  
51 and basically, everything is the same as original MM. Thus, there is no point in providing details such  
52 as the ones presented in Table 1.

53 According to Table 1, in minimal MM, except for one case, CartPole(4,4), the number of decision  
54 points and number of states are equal. Also, the number of decision points increases in many cases  
55 comparing to the original MM, which makes explainability capability more complex. As pointed  
56 out in the paper, Section 5.1, it is because minimal MMs integrate the decision points with unrelated  
57 states. This strongly obscures the ability to interpret agent's decision making process.

Table 1: MM results for control tasks and Atari environments.

Game	QBN Sizes		Original MM				Functional pruning				Minimal MM			
	$N_h$	$N_o$	Decis. Points	States	Obs.	Perf.	Decis. Points	States	Obs.	Perf.	Decis. Points	States	Obs.	Perf.
Acrobot	4	4	9	12	38	-77.1	2	4	3	-80.7	3	3	11	-80
	8	8	79	42	200	-77.1	2	4	5	-79.9	3	3	7	-86
CartPole	4	4	6	7	18	500	2	4	5	<b>500</b>	2	3	8	500
	8	8	7	8	58	500	2	4	5	<b>500</b>	3	3	11	500
Lunar Lander	32	32	195	1426	1150	180.48	184	1387	980	172.2	41	41	92	165
	32	64	249	1389	1437	204.93	230	1321	1327	197.35	19	19	73	147
Bowling	32	50	5	608	525	60	<b>0</b>	530	437	<b>60</b>	5	5	19	60
	64	100	5	630	552	60	<b>0</b>	546	488	<b>60</b>	3	4	12	60
Boxing	32	50	<b>0</b>	1274	1270	100	<b>0</b>	1274	1270	<b>100</b>	19	19	109	100
	64	100	<b>0</b>	1097	1095	100	<b>0</b>	1097	1095	<b>100</b>	14	14	101	100
Breakout	32	50	4	2479	2466	404	<b>0</b>	2365	2345	<b>404</b>	8	8	28	404
	64	100	5	1659	1608	404	<b>0</b>	1598	1540	<b>404</b>	11	11	43	404
MsPacman	32	50	43	728	716	3060	<b>0</b>	612	597	<b>3060</b>	21	21	70	3060
	64	100	34	895	876	3060	<b>0</b>	776	758	<b>3080</b>	9	9	45	3060
Pong	32	50	<b>0</b>	383	369	21	<b>0</b>	383	369	<b>21</b>	3	3	12	21
	64	100	2	384	369	21	<b>0</b>	271	268	<b>21</b>	4	4	10	21
SeaQuest	32	50	46	2167	2233	2580	<b>0</b>	1679	1577	<b>2580</b>	16	16	140	2580
	64	100	18	2244	2261	2580	<b>0</b>	1834	1883	<b>2580</b>	17	17	135	2580
Space Invaders	32	50	102	1700	1709	1820	<b>0</b>	1314	1350	<b>1820</b>	30	30	40	1820
	64	100	35	1914	1852	1820	<b>0</b>	1832	1802	<b>1820</b>	11	11	27	1820

## 58 6 Qualitative analyses

59 Since Moore Machines are large, we uploaded all of them here: <https://tinyurl.com/y96d8jub> for  
60 better understanding of their details.

### 61 6.1 Atari: Case Studies

62 **MsPacman.** The original MM for MsPacman with QBNs of size (64, 100) has 34 decision points  
63 before accounting for the warm-up and termination periods. After the reduction for warm-up and  
64 termination the MM is left with 19 decision points. We observed that most of the branches in the MM  
65 are visited only once and any single state transition is covered no more than 4 times during an episode.  
66 This indicates that little high-level generalization of the strategy is occurring. We considered the  
67 differential saliency at all decision points and show one example in Figure 1a. The saliency primarily  
68 focuses on the middle of the map at a location which distinguishes the presence of Pacman and less  
69 attention at a location distinguishing the presence of a ghost. By applying the functional pruning, we  
70 are able to remove all “non-strategic” branches from all decision points throughout the MM. This  
71 emphasizes that these salient features simply serve as arbitrary landmarks with no strategic value.  
72 This left us with an open-loop controller with no drop in performance. In fact, performance improved  
73 by 20 points.

74 The pruned MM, depicted in Figure 1b, gives the insight that agent’s policy is a pruned open-loop  
75 policy. The edges with two parallel lines indicate the start-up and termination phases of the game,  
76 which is an interpretable reduction introduced in the paper. On the other hand, the minimal MM,  
77 shown in Figure 1c, gives no insights about the agent’s behavior. Since semantically unrelated  
78 states are matched to each other, complexity is even increased. Figure 2 shows an example of this  
79 introduced complexity. All four frames in Figure 2 are outgoing observations of a decision point,  
80  $S_3$ , in the minimal MM. As it can be seen, these observations are semantically distinct to humans.  
81 Figure 2a shows a frame early in the game, where there are lots of rewards available and ghosts  
82 are not out completely. Figure 2b and c show a frame in the middle of the game. In b, Pacman  
83 is not being threatened by any ghosts, but in c there is a very close ghost to it. Figure 2d shows a  
84 frame from almost end of the game where rewards are sparse. Although these frames encode very  
85 different semantics, but minimal MM treats them semantically related, which is misleading in terms  
86 of interpretation.



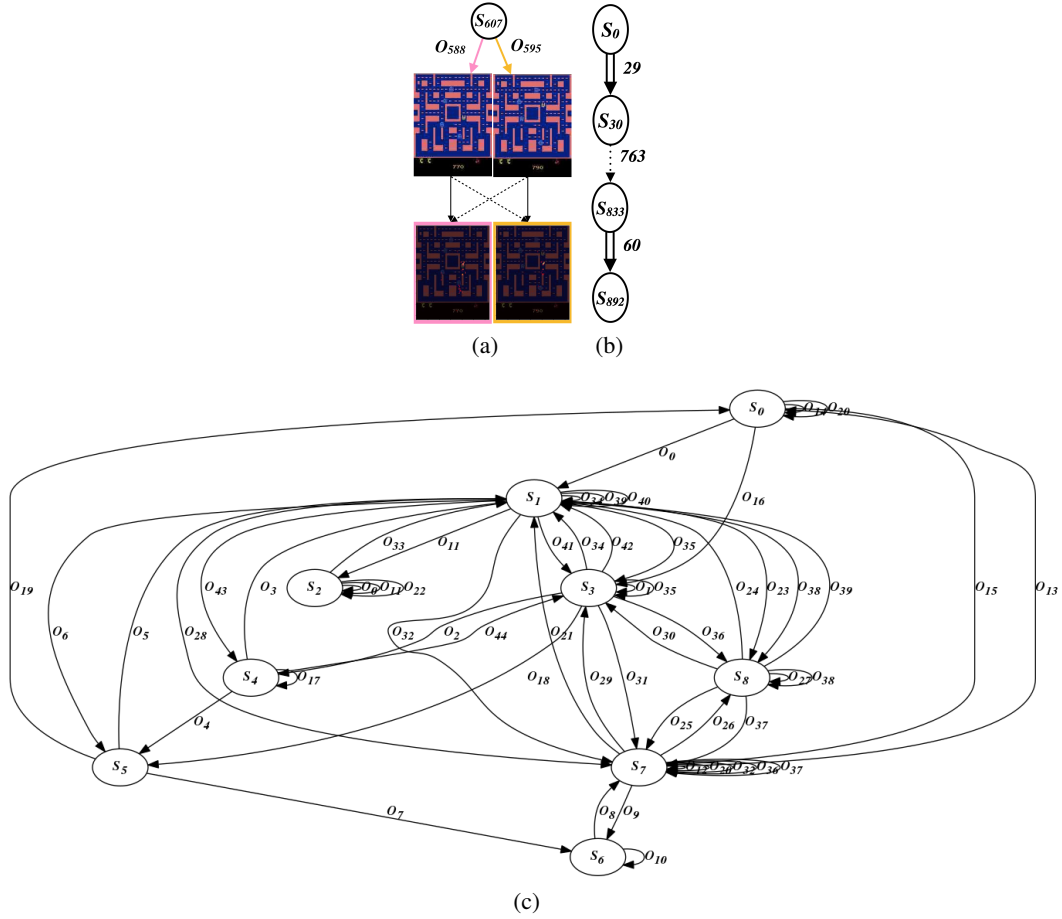


Figure 1: MsPacman: a) Differential saliency for a sample decision point. The first row shows a sample observation that occurs for each branch. The second row gives differential saliency for pairs of observations (dotted arrows indicate the baseline), b) pruned MM, c) minimal MM.

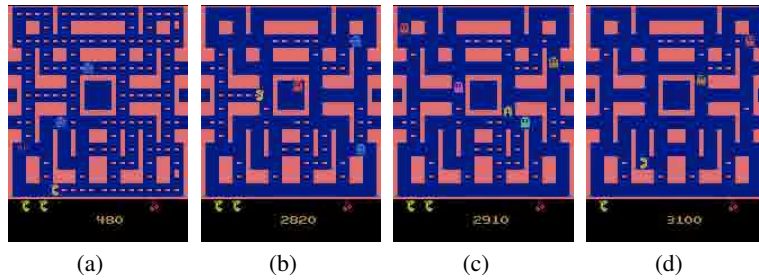


Figure 2: Different observations as branches of decision point  $S_3$  in minimal MM.

87 **Breakout.** QBN pair of (64, 100) is considered in this game as well. In Figure 3a, pruned MM, and  
 88 in Figure 3b, minimal MM can be seen. Breakout's policy turned out to be a pruned open-loop policy,  
 89 but this could not be possibly understood by looking at the minimal MM. In fact, it is hard to get any  
 90 explanation about policy based on minimal MM.

91 Figure 4 shows four semantically different observations that are turned into branches of a state in the  
 92 minimal MM. This set of various observations are the outgoing branches of decision point  $S_9$  in the  
 93 corresponding minimal MM.

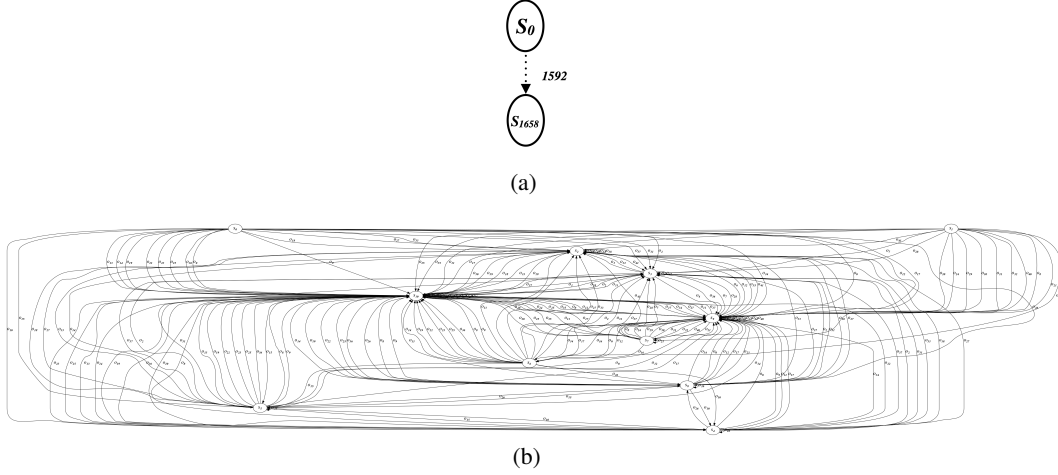


Figure 3: Breakout: a) pruned MM, b) minimal MM.

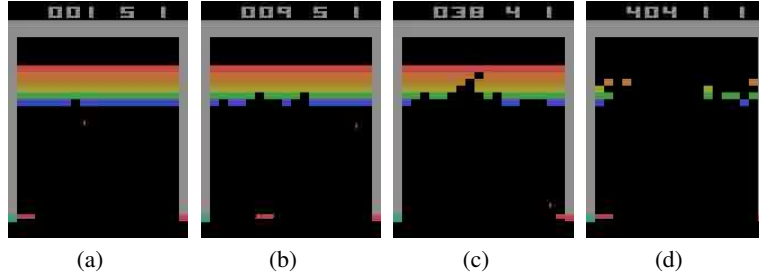


Figure 4: Different observations as branches of decision point  $S_9$  in minimal MM.

94 **Other games (Boxing, SeaQuest, SpaceInvaders).** Similar scenario happens in all other environ-  
 95 ments as well. As an example, we consider Boxing. Figure 5 shows the pruned MM and minimal MM,  
 96 where minimal MM looks tangled and very hard to decode. Pruned MM looks like a straight path,  
 97 which shows that at key decision points, policy does not strategically rely on observations, instead it  
 98 relies on memory. Figure 6 shows four different observations as branches of  $S_5$  in the minimal MM.  
 99 Figure 6a is where agent is hitting the opponent, Figure 6b agent is being hit, and in Figure 6c and d  
 100 there is a distance between the two players. This shows how different each observation is, in terms of  
 101 interpretation. But minimal MM counts them as semantically relevant states which is misleading.  
 102 Figure 7 and Figure 8 demonstrate similar properties for SeaQuest. And Figure 9 and Figure 10  
 103 illustrate them for SpaceInvaders.

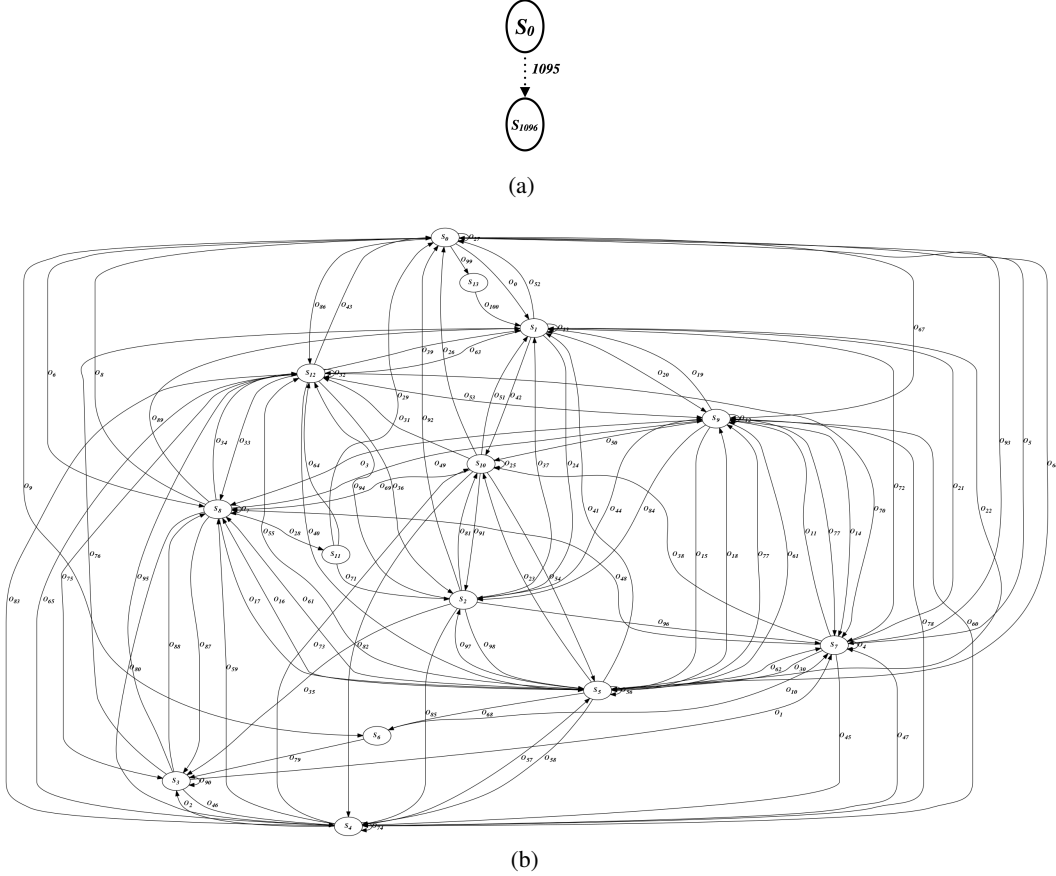


Figure 5: Boxing: a) pruned MM, b) minimal MM.

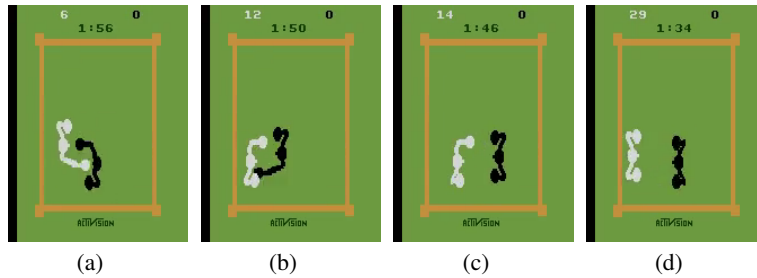


Figure 6: Different observations as branches of decision point  $S_5$  in minimal MM.

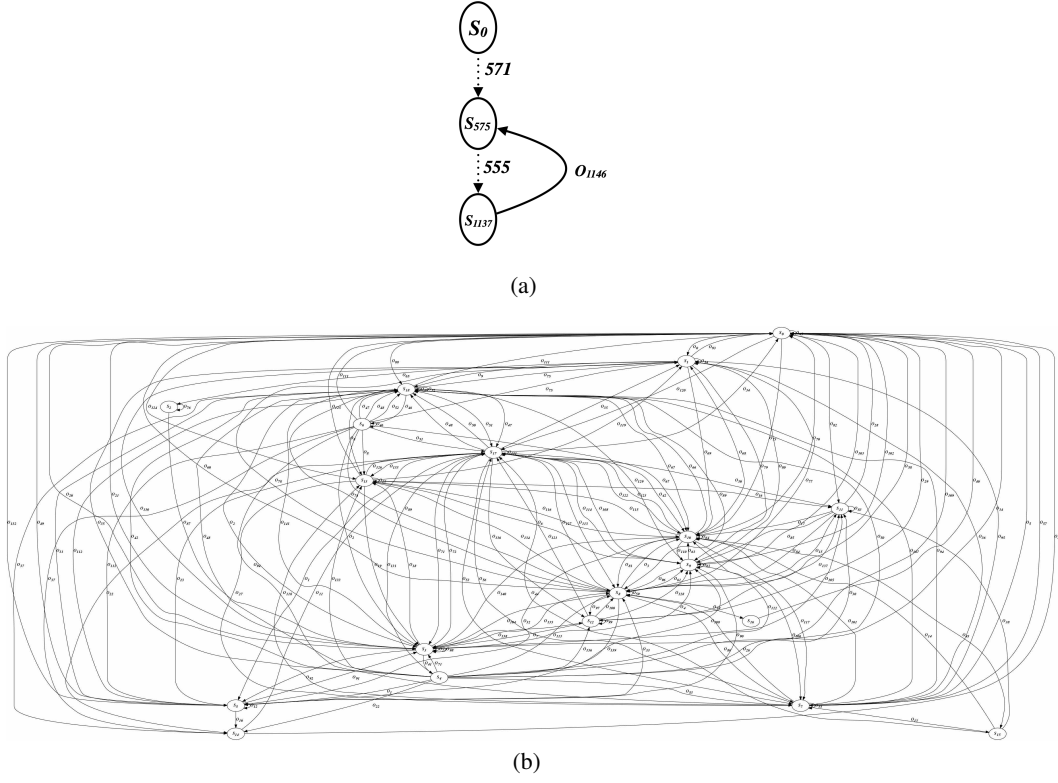


Figure 7: SeaQuest: a) pruned MM, b) minimal MM.

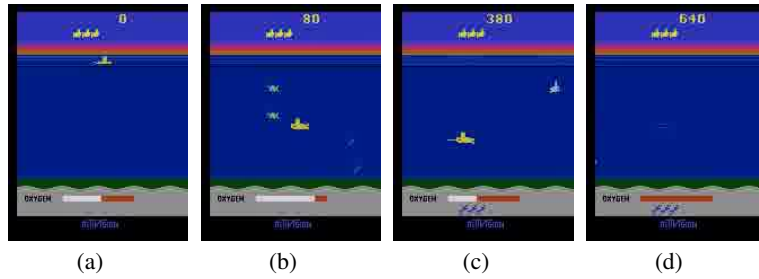


Figure 8: Different observations as branches of decision point  $S_6$  in minimal MM.

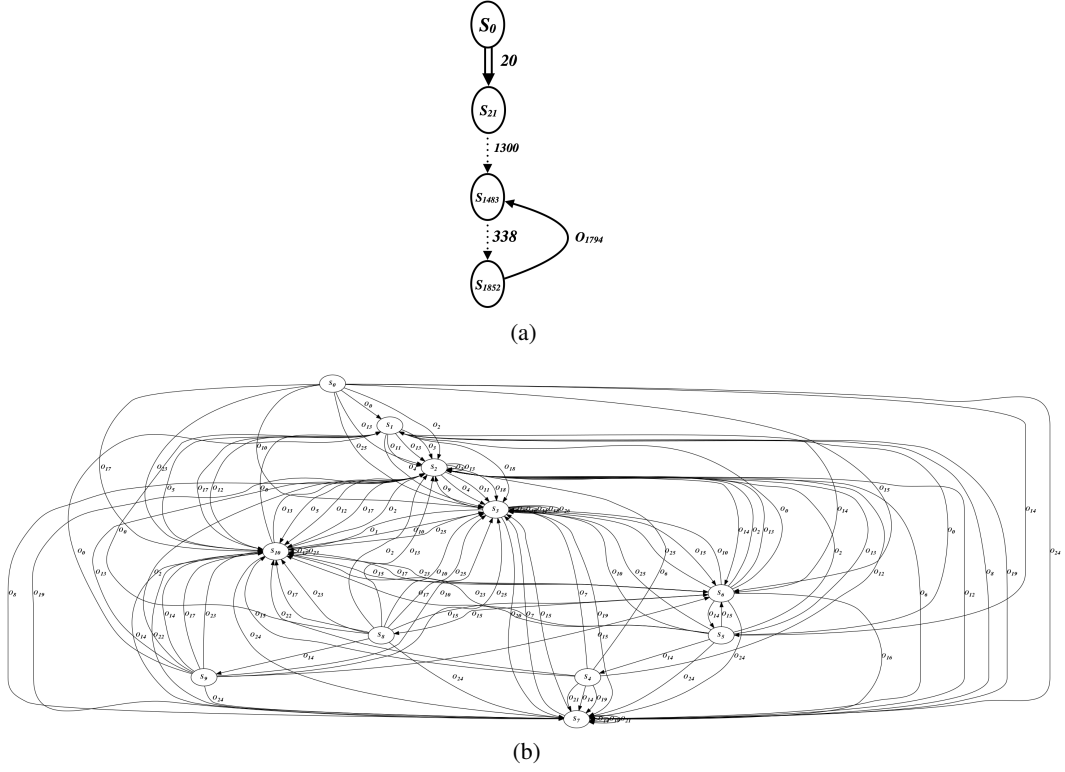


Figure 9: SeaQuest: a) pruned MM, b) minimal MM.

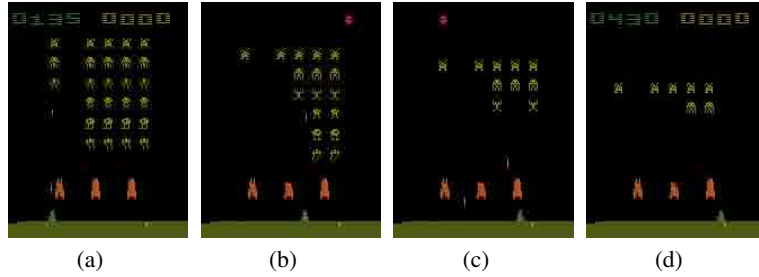


Figure 10: Different observations as branches of decision point  $S_6$  in minimal MM.

## 6.2 Stochastic Classic Control Tasks

**LunarLander.** This task involves landing a rover using actions that fire one of three thrusters: main, left, right, and no-op. The MMs for both QBN pairs were significantly larger than for the other continuous control tasks, likely due to increased complexity and stochasticity. Functional pruning was not significantly effective, according to Table 1. We analyzed many of these decision points and found that the “distance to the ground” is usually the most salient feature across decision points. One exception is the initial decision point, shown in Figure 11. We focus on branching observations of  $O_0, O_{379}, O_{831}$  which lead to states having different fire actions *main engine*(A2), *right engine*(A3) and *left engine*(A1), respectively. The saliency comparison of these observations show prime differences in x-velocity and y-velocity, thereby opposite direction engines are fired to stabilize the rover. This decision point does not attend to rover coordinates (x,y position) and leg-positions, which are more relevant when the lander is closer to the ground.

Regarding the minimal MM, due to its big size, it was not possible to be added here. Minimizing MM adds a lot of unexpected and unfavorable complexities to the MM, which makes it uninterpretable, while giving no information on agent’s behavior. Functional pruning does not provide much insights into the MM of LunarLander, but our proposed differential saliency tool gives very interesting insights. To the best of our knowledge, this level of insight has not been given in any prior work.

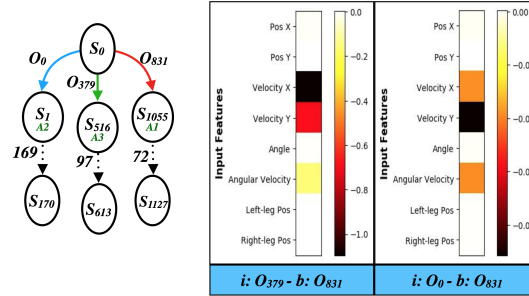


Figure 11: Pruned MMs for LunarLander. Next to the pruned MM it the saliency of features for first decision point. For each saliency map, input image and baseline image are shown.